Biochemical and Biophysical Research Communications 446 (2014) 1096–1101

Contents lists available at ScienceDirect

Biochemical and Biophysical Research Communications

journal homepage: www.elsevier.com/locate/ybbrc

TMEM16A alternative splicing isoforms in *Xenopus tropicalis*: Distribution and functional properties

A. Huanosta-Gutiérrez, A.E. Espino-Saldaña, J.P. Reyes, A. Pétriz, R. Miledi, A. Martínez-Torres *

Departamento de Neurobiología Celular y Molecular, Laboratorio de Neurobiología Molecular y Celular, Instituto de Neurobiología, Campus UNAM Juriquilla, Querétaro, Qro CP 76230, Mexico

ARTICLE INFO

Article history:
Received 8 March 2014
Available online 21 March 2014

Keywords:
Anoctamin 1
Calcium-activated chloride channels
Splice isoforms

ABSTRACT

Oocytes of *Xenopus tropicalis* elicit a Ca^{2+}-dependent outwardly rectifying, low-activating current ($I_{Cl,Ca}$) that is inhibited by Cl^- channel blockers. When inactivated, $I_{Cl,Ca}$ shows an exponentially decaying tail current that is related to currents generated by TMEM16A ion channels. Accordingly, RT-PCR revealed the expression of five alternatively spliced isoforms of TMEM16A in oocytes, which, after expression in HEK-293 cells, gave rise to fully functional Cl^- channels. Upon hyperpolarization to −80 mV a transient current was observed only in isoforms that carry the exon 1d, coding for two potentially phosphorylatable Threonine residues. The identified isoforms are differentially expressed in several tissues of the frog. Thus, it appears that *X. tropicalis* oocytes express TMEM16A that gives rise to a Ca^{2+}-dependent Cl^- current, which is different from the previously reported voltage-dependent outwardly rectifying Cl^- current.

1. Introduction

Oocytes of amphibians elicit a number of voltage-activated membrane currents, including a current known as $I_{Cl,Ca}$, which is generated by Ca^{2+}-dependent Cl^- channels (CaCC). In *Xenopus laevis*, I_{ClCa} is generated by activation of the channel-forming protein TMEM16A (Ano1) [1–4]. In this species, the CaCC underlie a transient outward current (T_{out}) [5] and is important for the prevention of polyspermy [6]. Recent observations in the amphibian experimental model *Xenopus tropicalis* disclosed that the frog's oocytes generate an outwardly rectifying Cl^- current composed of three functionally and pharmacologically distinguishable components: a voltage-activated, Ca^{2+}-independent current probably due to activation of the voltage-dependent ClC5 channel-and two Ca^{2+}-dependent Cl^- currents: one is generated by the activation of TMEM16A channels, while the origin of the second one remains uncertain [1].

Nevertheless, only a fraction (5–10%) of *X. tropicalis* oocytes showed T_{out} currents like those recorded in *X. laevis* (this may be due to a small Ca^{2+} influx through voltage-operated calcium-channels; VOCC), even though RT-PCR revealed the expression of TMEM16A mRNA [1]. This latter result provides an explanation for one of the Ca^{2+}-dependent Cl^- currents and the oscillatory Cl^- responses generated by activation of G protein-coupled receptors in these cells [7]. Furthermore, sequencing of the TMEM16A open reading frame isolated from *X. tropicalis* oocytes revealed multiple isoforms generated by alternative splicing, potentially increasing the functional diversity of the CaCC.

This report aims to determine the properties of the endogenous CaCC from *X. tropicalis* oocytes and to characterize the TMEM16A isoforms by functional expression in HEK-293 cells, as well as to determine the tissue distribution of these isoforms.

2. Materials and methods

2.1. Recordings in X. tropicalis oocytes

All animals were handled in accord with the guidelines of the National Institutes of Health Guide for Care and Use of Laboratory Animals and with the approval of the National University of Mexico. Stage V–VI oocytes were harvested as previously described [1]. Ovarian lobes were removed, and oocytes were manually isolated and kept at 16 °C in Barth's solution. Electrophysiological recordings were carried out 1–3 d after isolation.

Abbreviations: A-9-C, anthracene-9-carboxylic acid; ANO1, anoctamin 1; DIDS, 4,4′-diisothiocyano-2,2′-stilbenedisulfonic acid; DMSO, dimethyl sulfoxide; $I_{Cl,Ca}$, calcium-activated chloride current; NFA, niflumic acid; VOCC, voltage-operated calcium channels; xtTMEM16A, *Xenopus tropicalis* TMEM16A protein.

* Corresponding author. Fax: +52 442 238 1064.
E-mail address: ataulfo@unam.mx (A. Martínez-Torres).

http://dx.doi.org/10.1016/j.bbrc.2014.03.057
0006-291X/

Currents were recorded by the two-electrode voltage-clamp technique. Ringer's solution with 10 mM Ca^{2+} was used to increase Ca^{2+} influx into the oocyte through the seemingly few VOCC. Partial substitution of Ca^{2+} by 10 mM Mn^{2+} blocked the current by about 50% (Supplementary Fig. 1). The voltage protocol used for the characterization consisted of 500-ms steps from −80 to 120 mV in increments of 20 mV, followed by a 250-ms repolarization to −60 mV (holding potential was −60 mV).

2.2. Cloning, heterologous expression, and distribution of xtTMEM16A variants

The complete coding sequence for xtTMEM16A was amplified from oocyte RNA with specific primers and cloned into pGEMT-Easy [8]. Five alternative splice variants were identified (GenBank accession KF983358, KF983359, KF983360, KF983361, and the previously reported KF747702). For expression in mammalian cells, each splice variant was introduced in pcDNA3 (Invitrogen™) or pEFGP-N1 (Clontech).

Heterologous expression and whole-cell patch-clamp recordings were performed in HEK-293 cells as described previously [8]. The voltage protocol used for the characterization consisted of 1-s steps from −100 to 140 mV in 30-mV increments, followed by a 1-s repolarization to −100 mV (holding potential was −60 mV). To visualize the distribution of TMEM16A in *X. laevis* oocytes, a GFP-tagged isoform (xtTMEM16A(13)) was injected into the nucleus, and the expression was assessed 72 h later, under a LSM 510 META Zeiss microscope with an EC Plan-Neofluar 20×/0.5 M27 objective, using 488 nm for GFP excitation.

For membrane labeling, 24 h after transfection the HEK cells were incubated at 0 °C for 1 min with 20 μg/ml of FM® 4-64FX (Molecular Probes®) diluted in Hank's balanced salt solution (HBSS) without Mg^{2+} or Ca^{2+}. Images were obtained with the same microscope and a 40×/NA 1.35 oil immersion objective, using 561 nm for excitation of FM 4-64FX and 488 nm for GFP excitation. The optical slice was set to 2 μm. Data analysis was performed using *Image J* software 1.48g (National Institutes of Health).

To determine the distribution of alternatively spliced exons of xtTMEM16A, a set of primers was designed to amplify overlapped fragments based on the sequence previously reported (gi|194332620 and gi|574460278). RNA was obtained from oocytes and brain tissue, and cDNAs were amplified using the SS®III One-Step RT-PCR kit (Invitrogen™). Amplicons were cloned into pGEMT-Easy vector and sequenced. Specific primers were designed to identify the pattern of alternative splicing (Supp. Table 1).

2.3. Solutions

For the pharmacological characterization of the oocyte CaCC, Cl^- channel blockers A-9-C, DIDS, and NFA were added to normal bath solution to final concentrations of 3, 10, 30, 100 and 300 μM by appropriate dilutions of the respective DMSO stock solutions. DMSO had no effect on the oocyte currents.

2.4. Data analysis

Data are expressed as mean ± SEM. In all cases, n denotes the number of cells tested, and *N* indicates the number of frogs tested. Time constants of activation and deactivation (T_{act} and T_{deact}) were calculated from whole-cell records by fitting a single exponential, either to activating currents at +100 mV or to tail currents at −100 mV. To evaluate any difference in the currents activated by the hyperpolarizing voltage pulses in the recordings of HEK-293 cells, we measured the ratio (I_{start}/I_{end}) of the current amplitude measured at the start (I_{start}), −100 mV, to the current measured at the end (I_{end}), −100 mV, (as indicated by the red arrows in Fig. 3B). Dose–response relationships for current inhibition by A-9-C, DIDS, and NFA are shown normalized to the maximal current amplitude in the absence of blocker. The half-inhibitory concentration (IC_{50}) was estimated as described previously [1]. Statistically significant differences between groups were assessed by a one-way ANOVA followed by the Bonferroni multiple comparison *post hoc* test ($P < 0.05$).

3. Results

3.1. A CaCC current in X. tropicalis oocytes

Oocytes of *X. tropicalis* mostly show passive currents upon depolarization of the plasma membrane. In contrast, when *X. laevis* oocytes are stepped to +20 mV, a T_{out} current driven by CaCC is elicited [5,9]. Following this protocol, we found that only 5–10% of the *X. tropicalis oocytes tested* generate this T_{out} current [1], although a CaCC is commonly found in oocytes of this species [7]. Thus, to increase the entry of Ca^{2+} through VOCC, we increased the concentration of this cation to 10 mM, a strategy previously shown to be successful in revealing the T_{out} current [9]. In this condition, stepping the plasma membrane from −60 mV to +120 mV generated a slow activating current (τ_{act} = 188.39 ± 12.68 ms) in oocytes of most donors examined (Fig. 1A). The current was voltage dependent and outwardly rectifying, and it rose almost linearly from +80 mV onward, reaching amplitudes from 20.9 ± 2.1 nA to 54.5 ± 4.1 nA at +120 mV; this current was readily inhibited when Ca^{2+} was partially substituted by Mn^{2+} in the Ringer buffer (see Supplementary Figure 1). Importantly, this current showed an exponentially decaying tail current upon inactivation, a characteristic of CaCC [10]. In addition, when consecutive depolarization steps to +120 mV were applied to oocytes bathed in 10 mM Ca^{2+} Ringer, the current showed only little desensitization.

We then tested the sensitivity of the natively expressed CaCC in the oocytes to several Cl^- channel blockers, namely A-9-C, DIDS, and NFA. We observed a partial inhibition (Fig. 1B–D) of the endogenous CaCC with all blockers, but the current was not completely abolished as reported before [11], probably due to the presence of the Ca^{2+}-independent Cl^- current recently discovered in oocytes of *X. tropicalis* [1]. Dose–response curves were constructed for each blocker (Fig. 1E). The IC_{50} values were: DIDS (52.9 μM), NFA (57.9 μM), and A-9-C (66.3 μM).

3.2. Cloning and alternative splicing of X. tropicalis TMEM16A

The results shown above corroborated the presence of CaCC in *X. tropicalis* oocytes, and our previous experiments showed the expression of TMEM16A mRNA in these cells [1]. After sequencing ten independent clones from oocytes and ten from brain, we found five different alternatively spliced isoforms; the alternative splicing involves four exons that are named according to the corresponding exon in human [4], namely 1b, 1d, 13, and 15 (shown schematically in Fig. 2A). It is interesting that sequence of the alternatively spliced exons 1b and 1d have no homolog in the human TMEM16A (see Supplementary Fig. 2). Instead of the characteristic EAVK sequence found in humans, the *X. tropicalis* homolog codes for a GMVK sequence. In addition, exon 1d codes for a sequence with two potentially phosphorylatable threonine residues that may confer different properties to the channel.

Since splice variants of the xtTMEM16A protein may have distinct characteristics optimized for the requirements of various tissues and cells at different stages of development, we carried out experiments aimed to gain insight into the pattern of alternative splicing in different tissues, as well as in oocytes (Fig. 2B). Specific mRNA regions were amplified to determine the expression or

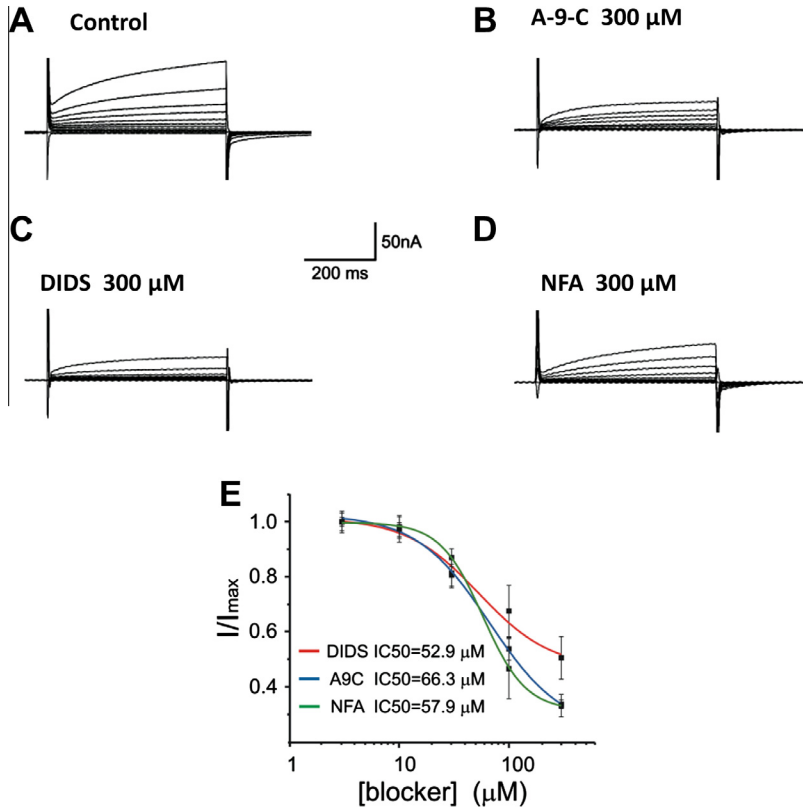

Fig. 1. Properties of CaCC natively expressed in *X. tropicalis* oocytes. (A–D) Representative current traces upon application of the voltage protocol described in Section 2 from oocytes bathed in external solution containing 10 mM Ca^{2+} or the indicated blockers (300 µM). (E) Dose–response curve for each channel blocker ($n = 5$; $N = 4$). Current is normalized. Data points are means ± SEM.

absence of expression of alternatively spliced exons 1b, 1d, 13 and 15.

Expression of exon 1b was observed in most tissues except liver and lung, although it is present at a low level in skeletal muscle, small intestine, and oocytes. Isoforms lacking exon 1d predominate in almost all organs; in fact, this exon is absent in brain, liver, and muscle. In the case of exon 13, both variants, including and skipping the exon, were detected only in brain and skeletal muscle, similar to the case in human [12]. Exon 15 was present in all organs with some variability, as observed in human and mouse. In oocytes, the isoform skipping this exon was not detected, but since we found it in two of the five isoforms cloned from oocytes, it must be absent in only a small proportion of mRNAs. We did not see detectable differences in the expression pattern among oocytes at different stages of development (data not shown). From these results, we can conclude that TMEM16A (13, 15) is the predominant isoform expressed in oocytes, followed by (1d, 13, 15) and (1b, 13, 15).

To gain some insight about the cellular distribution of TMEM16A, cDNA for the TMEM16A (13) isoform was fused to GFP [8] (Fig. 3A). This chimera partially co-localized with FM4-64 in the plasma membrane of transfected HEK cells, which contrasted with the cytosolic localization of soluble GFP (Fig. 3A and Supplementary Video 1a,b). In addition, some vesicular xtTMEM16A (13)-GFP was also identified, which may suggest some role for the protein channel in intracellular signaling, or it may reflect the natural trafficking of the protein from the endoplasmic reticulum.

The oscillatory Cl^- current generated in oocytes may be due to the distribution pattern of TMEM16A along the plasma membrane that receives the Ca^{2+} waves released from the endoplasmic reticulum; the distribution of CaCC has been described as asymmetrical in *X. laevis oocytes*, with larger Cl^- currents evoked towards the animal hemisphere [9]. Thus, to determine whether TMEM16A is differentially distributed in the plasma membrane, we injected the xtTMEM16A(13) cDNA tagged with GFP into *X. laevis* oocytes, and found that the fluorescent protein is located mostly towards the animal hemisphere, whereas only a faint label was detected in the vegetal hemisphere (Supplementary Fig. 3). This result is consistent with the differential distribution of the CaCC recorded electrophysiologically [9].

3.3. Properties of xtTMEM16A isoforms expressed in HEK cells

The five xtTMEM16A isoforms, namely: 1: (13); 2: (1d, 13); 3: (13, 15); 4: (1b, 13, 15); 5: (1d, 13, 15) formed fully functional channels when expressed in HEK-293 cells. Representative traces of current generated by CaCC formed by the different xtTMEM16A isoforms are shown in Fig. 3B; they are voltage dependent and show an activation at positive membrane potentials. There were no differences among the variants with regard to the time-dependent course of activation during a strongly depolarizing step (activation) and the time-dependent course of tail current decrease during the repolarization step (deactivation) (Supplementary Fig. 4). However, in all clones that include exon 1d (i.e., xtTMEM16A (1d, 13) and (1d, 13, 15)), a hyperpolarizing step from the holding potential to −100 mV resulted in a transient current (Fig. 3B), probably due to a group of channels which are open at the holding potential and that gradually become closed at the voltage of −100 mV (*i.e.*, a tail current). Thus, current amplitudes were measured at the beginning of the step (peak of the tail current; I_{start}) and at the end of the step (I_{end}), and the ratio (I_{start}/I_{end}) denotes the magnitude of the tail current elicited by the −100 mV step. As shown in Supp. Table 2, the ratios (I_{start}/I_{end}) of xtTMEM16A (1d, 13) (2.25 ± 0.09) and (1d, 13, 15) (1.5 ± 0.11) are significantly different from those of other isoforms.

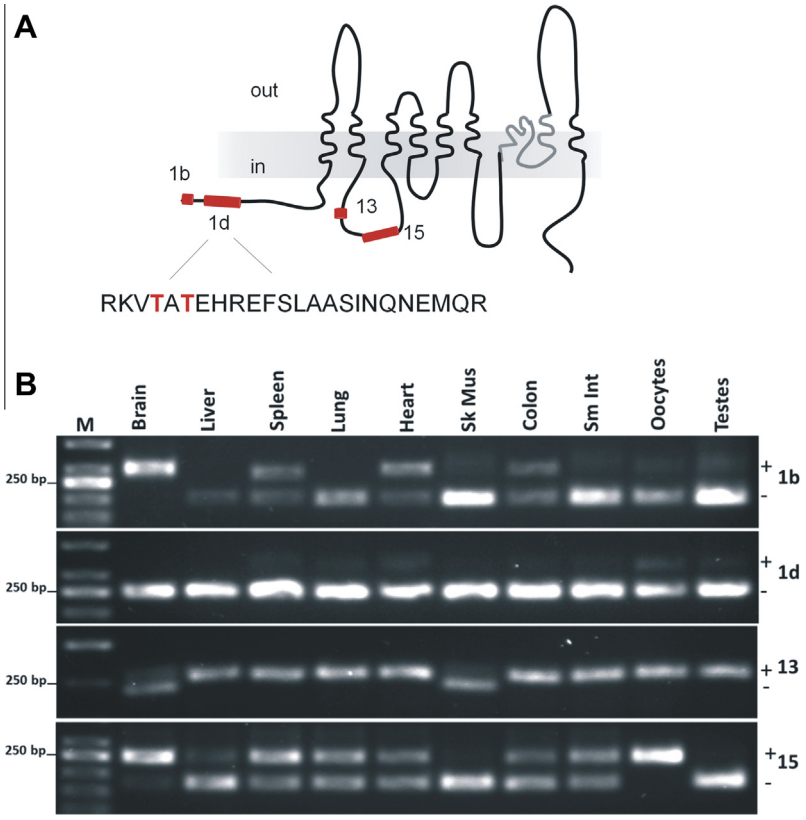

Fig. 2. Alternatively spliced variants of xtTMEM16A. (A) Topological model of xtTMEM16A. The four segments that can be alternatively spliced are shown in red. The amino acid sequence of exon 1d is shown as an inset. The Thr residues indicated in red are potential targets for phosphorylation. (B) Distribution of xtTMEM16A. Nine different tissues and oocytes were screened for the expression of xtTMEM16A exons 1b, 1d, 13, and 15. Sk Mus, Skeletal muscle; Sm Int, small intestine. (For interpretation of the references to color in this figure legend, the reader is referred to the web version of this article.)

4. Discussion

The experiments described here reveal an outwardly rectifying Cl^- current in *X. tropicalis* oocytes that has properties of the TMEM16A protein channels. This current is part of a tripartite set of voltage-dependent Cl^- conductances generated upon depolarizing the plasma membrane of the oocyte: one component is Ca^{2+} independent and two are Ca^{2+} dependent. The Ca^{2+}-independent Cl^- current is mostly due to the expression of ClC-5 [1], whereas one of the Ca^{2+}-dependent components results from the activation of TMEM16A (mainly recognized by the tail currents induced after repolarizing the plasma membrane to −60 mV); the third component is yet to be identified.

The CaCC current of oocytes is partially inhibited by Cl^- channel blockers at concentrations well within the range reported previously by others: 16–250 μM for DIDS, 2–44 μM for NFA, and 10–1000 μM for A-9-C [10]. However, it was consistently determined that the outward current was not totally blocked by these compounds, probably due to the appearance of several other endogenous conductances; these include the Ca^{2+}-independent outwardly rectifying Cl^- current, and they could lead to misinterpretations of the results. We suggest that other, still unidentified, endogenous CaCC, expressed in *X. tropicalis* oocytes but not related to TMEM16A, may also determine the pharmacological profile of I_{ClCa} [1].

The gene structure of *X. tropicalis* TMEM16A is similar to that in other species [12,13]. Exons 13 and 15 of *X. tropicalis* are alternatively spliced, and the expression pattern of these exons in different tissues and organs is very similar to that described in human and mouse. However, the other alternatively spliced exons of *X. tropicalis*, 1b and 1d, do not have homologs in human or mouse. Interestingly, the protein segments coded by these exons are located in the intracellular N-terminus of the protein, which is a highly variable region. The N-terminus of mammalian TMEM16A is important for dimerization of the protein and for its calmodulin regulation site [14], and these sites seem to be well preserved in *X. tropicalis*.

We examined the kinetics of the five splice variants and found no evident differences with regard to activation and deactivation kinetics. However, xtTMEM16A (1d, 13) and (1d, 13, 15) showed a transient current when the membrane was brought to −100 mV, indicating that a significant population of channels is open at the holding potential (−60 mV) and closed after the membrane is hyperpolarized. The inclusion of exon 1d may account for this functional property since it adds two extra Thr residues that could be potentially phosphorylated, as these residues fit the consensus sequence for phosphorylation by cAMP- and cGMP PKC and Casein Kinase II. The diversity of isoforms derived from alternative splicing found in *X. tropicalis* TMEM16A does not immediately suggest an impact on the functional properties of the protein, and more structure/function assays are necessary to identify the subtle differences among the isoforms, such as the different Ca^{2+}-dependent kinetics of activation described previously [12].

Regarding the distribution of TMEM16A (13) within transfected HEK cells, it was expected that the fluorescence would be found in the plasma membrane but, remarkably, a considerable amount of protein was also detected in intracellular compartments. This observation contrasts with that of Vocke et al. [15], who detected TMEM16A-GFP mostly along the plasma membrane. Our observation may suggest an undisclosed intracellular role for TMEM16A, probably as a tethering protein between the endoplasmic reticulum and the plasma membrane, a role that has already

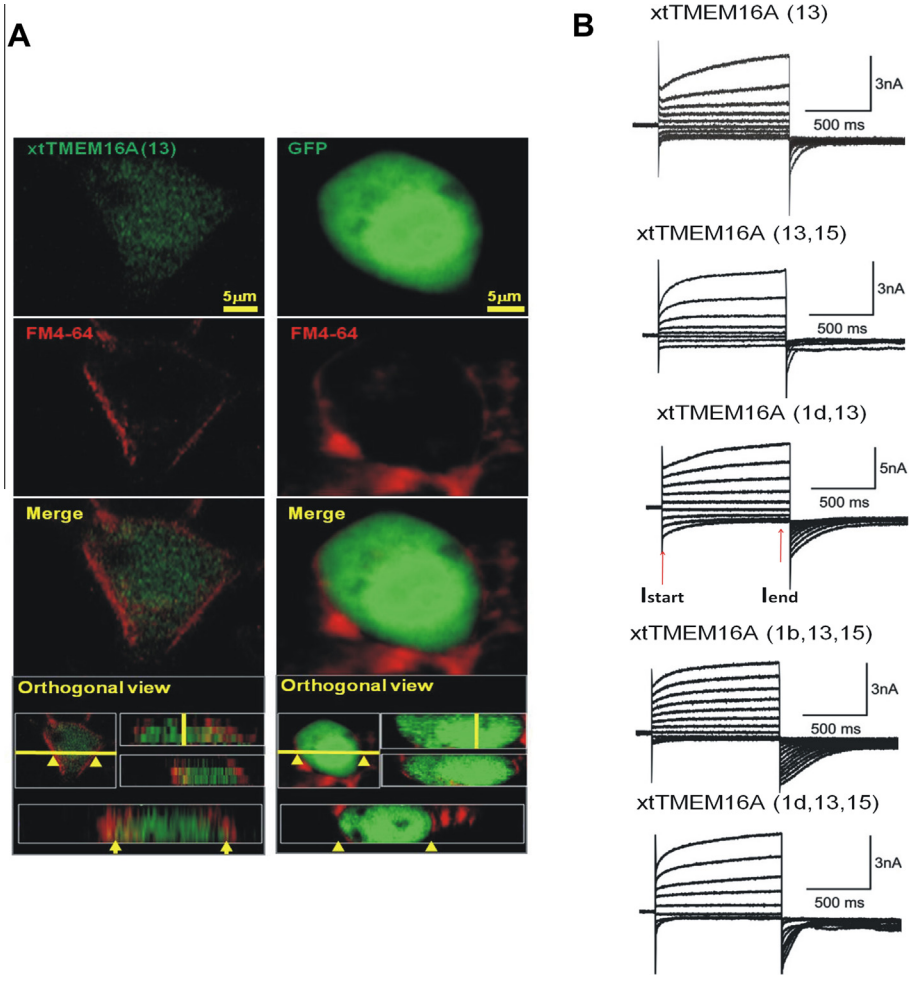

Fig. 3. (A) GFP-fused xtTMEM16A (13) partially co-localized with FM4-64 in the plasma membrane of transfected HEK cells (*arrows*); GFP fluorescence did not localize on the cell surface (*arrowheads*). Orthogonal view (*yellow lines*) outline the differences in the GFP and xtTMEM16A (13). Scale bar = 5 μm (B) Sample currents of the five isoforms showing the time courses of current activation and deactivation upon application of the voltage protocol described in Section 2. The red arrows indicate the amplitudes of the current measured at the start (I_{start}), −100 mV, and the current measured at the end (I_{end}), −100 mV, used to calculate the ratio (I_{start}/I_{end}). (For interpretation of the references to color in this figure legend, the reader is referred to the web version of this article.)

been described for the yeast *Ist-2* gene, an ortholog of the vertebrate TMEM16 family [16].

Finally, the results described here about the exon structure, tissue-specific alternative splicing patterns, and electrophysiological properties of CaCC formed by TMEM16A in *X. tropicalis* may be an important advance towards understanding the roles of this protein.

Acknowledgments

A.H.G. and A.P. are doctoral students from Programa de Doctorado en Ciencias Biomédicas, Universidad Nacional Autónoma de México (UNAM) and were supported by fellowships 335550 and 3347009 from CONACYT, respectively. This work was supported by Grants from; PAPIIT-DGAPA (A.M.T.) and PAPIIT IA201413 (J.P.R.). We appreciate the technical support from A. Antaramian and A. González from Unidad de Proteogenómica (I.N.B.) and N. Hernández-Ríos from Unidad de Microscopía (I.N.B.). We thank Marina Ramírez Romero for her technical assistance. We are grateful to Dr. D.D. Pless who edited the manuscript.

Appendix A. Supplementary data

Supplementary data associated with this article can be found, in the online version, at http://dx.doi.org/10.1016/j.bbrc.2014.03.057.

References

[1] L.D. Ochoa-de la Paz, A.E. Espino-Saldana, R. Arellano-Ostoa, J.P. Reyes, R. Miledi, A. Martinez-Torres, Characterization of an outward rectifying chloride current of *Xenopus tropicalis* oocytes, Biochim. Biophys. Acta 2013 (1828) 1743–1753.
[2] Y.D. Yang, H. Cho, J.Y. Koo, M.H. Tak, Y. Cho, W.S. Shim, S.P. Park, J. Lee, B. Lee, B.M. Kim, R. Raouf, Y.K. Shin, U. Oh, TMEM16A confers receptor-activated calcium-dependent chloride conductance, Nature 455 (2008) 1210–1215.
[3] B.C. Schroeder, T. Cheng, Y.N. Jan, L.Y. Jan, Expression cloning of TMEM16A as a calcium-activated chloride channel subunit, Cell 134 (2008) 1019–1029.
[4] A. Caputo, E. Caci, L. Ferrera, N. Pedemonte, C. Barsanti, E. Sondo, U. Pfeffer, R. Ravazzolo, O. Zegarra-Moran, L.J. Galietta, TMEM16A, a membrane protein associated with calcium-dependent chloride channel activity, Science 322 (2008) 590–594.
[5] R. Miledi, A calcium-dependent transient outward current in *Xenopus laevis* oocytes, Proc. R. Soc. Lond. B Biol. Sci. 215 (1982) 491–497.
[6] N.L. Cross, R.P. Elinson, A fast block to polyspermy in frogs mediated by changes in the membrane potential, Dev. Biol. 75 (1980) 187–198.
[7] J.S. Marchant, I. Parker, *Xenopus tropicalis* oocytes as an advantageous model system for the study of intracellular Ca(2+) signalling, Br. J. Pharmacol. 132 (2001) 1396–1410.
[8] J.P. Reyes, A. Lopez-Rodriguez, A.E. Espino-Saldana, A. Huanosta-Gutierrez, R. Miledi, A. Martinez-Torres, Anion permeation in calcium-activated chloride channels formed by TMEM16A from *Xenopus tropicalis*, Pflugers Arch. (2013) [Epub ahead of print].
[9] R. Miledi, I. Parker, Chloride current induced by injection of calcium into *Xenopus* oocytes, J. Physiol. 357 (1984) 173–183.
[10] C. Hartzell, I. Putzier, J. Arreola, Calcium-activated chloride channels, Annu. Rev. Physiol. 67 (2005) 719–758.
[11] M.M. White, M. Aylwin, Niflumic and flufenamic acids are potent reversible blockers of Ca^{2}(+)-activated Cl^{-} channels in *Xenopus* oocytes, Mol. Pharmacol. 37 (1990) 720–724.

[12] L. Ferrera, A. Caputo, I. Ubby, E. Bussani, O. Zegarra-Moran, R. Ravazzolo, F. Pagani, L.J. Galietta, Regulation of TMEM16A chloride channel properties by alternative splicing, J. Biol. Chem. 284 (2009) 33360–33368.
[13] K.E. O'Driscoll, R.A. Pipe, F.C. Britton, Increased complexity of Tmem16a/Anoctamin 1 transcript alternative splicing, BMC Mol. Biol. 12 (2011) 35.
[14] J. Tien, H.Y. Lee, D.L. Minor Jr., Y.N. Jan, L.Y. Jan, Identification of a dimerization domain in the TMEM16A calcium-activated chloride channel CaCC, Proc. Natl. Acad. Sci. USA 110 (2013) 6352–6357.
[15] K. Vocke, K. Dauner, A. Hahn, A. Ulbrich, J. Broecker, S. Keller, S. Frings, F. Mohrlen, Calmodulin-dependent activation and inactivation of anoctamin calcium-gated chloride channels, J. Gen. Physiol. 142 (2013) 381–404.
[16] A.G. Manford, C.J. Stefan, H.L. Yuan, J.A. Macgurn, S.D. Emr, ER-to-plasma membrane tethering proteins regulate cell signaling and ER morphology, Dev. Cell 23 (2012) 1129–1140.